Environmental Science Nano

PAPER

View Article Online
View Journal | View Issue

Cite this: *Environ. Sci.: Nano*, 2017, 4, 1981

Ecotoxicological assessment of nanoparticle-containing acrylic copolymer dispersions in fairy shrimp and zebrafish embryos†

Tamara S. Galloway, *[a] Yuktee Dogra,[a] Natalie Garrett,[b] Darren Rowe,[a] Charles R. Tyler,[a] Julian Moger,[b] Eva Lammer,[c] Robert Landsiedel,[d] Ursula G. Sauer,[e] Gertrud Scherer,[f] Wendel Wohlleben[g] and Karin Wiench *[h]

Nanoparticle-containing polymer dispersions are widely used, but little is known of their environmental effects. We studied the bioavailability, uptake, tissue localisation and effects of nanoparticle-containing acrylic copolymer (ACP) dispersions (mean nanoparticle sizes: 80 nm and 110 nm) in aquatic invertebrates (*Thamnocephalus platyurus*; fairy shrimp) and *Danio rerio* zebrafish embryos after aquatic exposures. Dietary exposure tests were enabled using *Casper* zebrafish that lack skin pigmentation allowing for bioimaging of uptake and internal distribution. Aqueous exposures of 1000 and 2500 mg L^{-1} 80 nm-ACP or 110 nm-ACP showed no acute toxicity in fairy shrimp or zebrafish, constituting a non-toxic classification according to the United Nations Globally Harmonised System of Classification and Labelling of Chemicals threshold (100 mg L^{-1}). Similarly, dietary exposures resulted in no ecotoxicological effects. In *Casper* zebrafish fed with 80 nm-ACP-spiked food, hyperspectral signals derived using coherent Raman scattering (CRS) indicated that test material was present in the intestine, and possibly in the liver, but not in other organs. CRS imaging indicated that the chemical composition of the yolk sac of an 80 nm-ACP exposed zebrafish (aquatic exposure) was altered, attributed to a change in lipid metabolism, although we could not confirm with certainty that the test material was physically present in the yolk sac. These results illustrate how CRS microscopy can be used to investigate the bioaccumulation of organic nanomaterials, provided that they induce hyperspectral profiles distinct from the biological samples. In conclusion, both 80 nm- and 110 nm-ACP dispersions are internalised through dietary exposure, but are not associated with significant toxic effects.

Received 4th May 2017,
Accepted 18th August 2017

DOI: 10.1039/c7en00385d

rsc.li/es-nano

Environmental significance

Few studies are available on potential ecotoxicological effects of organic nanomaterials. We examined acute aquatic effects of widely used, environmentally relevant nanoparticle-containing acrylic polymer dispersions. In fairy shrimp and zebrafish embryos, the test materials showed virtually no acute aquatic toxicity. Further, we investigated the uptake, bioavailability, and biodistribution of the acrylic polymers using coherent Raman scattering (CRS) microscopy. When zebrafish were fed with acrylic polymer-containing food, test material was present in the intestine, possibly in the liver, but not in other organs. CRS microscopy proved to be a promising method for ecotoxicological investigations, not requiring extensive preparation to the biological sample. In conclusion, we provide insight on ecotoxicological effects of organic nanomaterials and on suitable tools for their further investigation.

Introduction

The majority of research into the environmental toxicity of nanomaterials has focused on inorganic nanomaterials, such as metals, metal oxides, amorphous silica and carbonaceous nanomaterials, with less attention paid to organic nanomaterials, such as nanoparticle-containing polymer dispersions.[1] A major class of polymer dispersions are produced using acrylic esters. Acrylates contain vinyl groups, *i.e.* two carbon atoms that double bond to each other and that are directly attached to the carbonyl carbon. Due to the high reactivity of the double bond, acrylates easily form polymers.

[a] *College of Life and Environmental Sciences, University of Exeter, EX4 4QD, UK. E-mail: t.s.galloway@exeter.ac.uk*
[b] *College of Mathematical and Physical Sciences, University of Exeter, EX4 4QD, UK*
[c] *BASF Schweiz AG, Klybeckstrasse 141, CH-4057 Basel, Switzerland*
[d] *BASF SE, GB/TB - Z470, D-67056 Ludwigshafen, Germany*
[e] *Scientific Consultancy – Animal Welfare, Hallstattfeld 16, D-85579 Neubiberg, Germany*
[f] *BASF SE, E-EDE/QP, D-67056 Ludwigshafen, Germany*
[g] *BASF SE, RAA/OR - B7, D-67056 Ludwigshafen, Germany*
[h] *BASF SE, FEP/PC - Z470, 67056 Ludwigshafen, Germany*

† Electronic supplementary information (ESI) available: Supplementary information, SI-tables and SI-figures. See DOI: 10.1039/c7en00385d

Acrylic copolymers (ACPs) are important raw materials used in industrial processes. Millions of tons of polymer dispersions are used as binders in applications such as adhesives, paints, coatings, paper and paper board coating, nonwoven fabrics, carpets, construction materials, and textile finishing agents.[1–3]

In the few available studies, ACP dispersions have been shown to possess low toxicity in mammals. Oral administration of 2 g per kg body weight ACP dispersions to rats did not result in any signs of acute toxicity, mutagenicity or sensitising activity.[1] In a short-term inhalation toxicity study in rats (5 days of exposure; 6 h per day), two ACP dispersions (the one containing approx. 35% nanoparticles in the aerosol and the other no appreciable amount of nanoparticles) did not elicit any adverse effects up to aerosol concentrations of 10 mg m^{-3}. Hence, the higher proportion of nanoparticles in these polymer dispersions did not affect the outcome of the study.[1]

Hazard assessment of nanomaterials and nanotechnology-enabled products should take into account all relevant aspects of their life cycle and biological pathways from their initial synthesis, to commercial use and disposal.[4–7] The potential ecotoxicology of nanoparticle-containing polymer dispersions is of particular concern for aquatic organisms, since aquatic systems are the ultimate repository for released anthropogenic substances.[8] In receiving waters, the ecotoxicology of nanomaterials, including polymers, is largely governed by their intrinsic properties and the nature of the local environment, which influences interactions with suspended particulate matter and the extent of biological and abiotic degradation, agglomeration and aggregation.[9,10] An enhanced understanding of the potential effects of nanomaterials to aquatic species requires a comprehensive determination of their system-dependent properties in relevant environmental matrices, coupled with detailed information of their bioavailability, uptake and distribution within the biological tissues of appropriate species.

Very few studies are available addressing the potential environmental effects of nanoparticle-containing polymer dispersions released into the environment.[11] In tests performed for regulatory purposes, a spectrum of nanoparticle-containing polymer dispersions did not show ecotoxicological effects in fish, daphnia or algae upon short-term exposure (unpublished in-house data). The published data available for polymer nanocomposites do not indicate appreciable nanoparticle release or (eco-)toxicity of released fragments.[12–14] When solid acrylate polymers with embedded quantum dots, used in the lighting industry, were exposed to different environmental and biological simulant fluids, the leachates contained soluble metals derived from the quantum dots, but no free quantum dots or quantum dot-containing polymeric debris.[15] Commercial nanofiller composites submitted to chemical stresses as relevant in outdoor aging and/or mechanical forces mimicking sanding can release fragment polymer particles, with a fraction as colloidal nanoparticles,[16,17] but these did not lead to significant toxicity.[12,13,18]

The present study investigated the bioavailability, uptake, body tissue distribution and effects of nanoparticle-containing ACP dispersions to an aquatic invertebrate *Thamnocephalus platyurus* (fairy shrimp) and *Danio rerio* (zebrafish) after aquatic and dietary exposures. Test methods adopted were the *International Standardisation Organisation 14380:2011 Water quality determination of the acute toxicity to Thamnocephalus platyurus Crustacea*; *Anostraca*, (fairy shrimp)[19] and the *Organisation for Economic Co-operation and Development (OECD) Test Guideline (TG) 236 Fish Embryo Toxicity (FET) test*[20] using *Danio rerio* (zebrafish) embryos.

Thereby, the present study served to provide first insight on the potential acute aquatic toxicity of nanoparticle-containing polymer dispersions. Assessment of short-term aquatic toxicity in invertebrates and fish is a mandatory component of the base set of data requirements for ecotoxicity testing. In *Regulation EC No. 1907/2006 on the Registration, Evaluation, Authorisation, and Restriction of Chemicals (REACH)*,[21] information on short-term aquatic toxicity in invertebrates is generally required for substances manufactured or imported in quantities exceeding 1 ton per year. Information on acute fish toxicity is generally required if the annual tonnage exceeds 10 tons. As compared to the fish acute toxicity test (OECD TG 203),[22] the FET test serves the 3Rs principle to replace, reduce and refine animal testing[23] that has been implemented in *Directive 2010/63/EU on the protection of animals used for scientific purposes*.[24] Therefore, the FET test was selected for acute aquatic fish toxicity testing in the present study. Since the zebrafish embryos used in the FET test are not considered as 'independently feeding larval forms', the test, as far as the embryos are concerned, does not fall within the scope of Directive 2010/63/EU.[24,25] In zebrafish embryos the egg shell, the chorion, is transparent[26,27] and the developmental stages are well characterised and completed rapidly, *i.e.* within 120 h.[28–30] The fairy shrimp were selected for acute aquatic toxicity testing in invertebrates, since they lack a carapace and have an open circulatory system, allowing an unimpeded exchange of oxygen or chemicals, and they are sensitive indicators of environmental pollution.[31,32]

Further, dietary exposure studies were conducted using zebrafish fry. These studies served to investigate the uptake and bioavailability of ACP dispersions in fish. Information on the toxicokinetics of substances are equally relevant for regulatory hazard and risk assessment. However, to data there are no standardised test methods to investigate test material uptake or biodistribution in environmentally relevant species. In the present study, the dietary exposure studies used a mutant line of *D. rerio*, known as *Casper*, whose embryos and adults lack all melanocytes and iridophores[33] avoiding problems associated with pigments that can interfere with the microscopic detection of internalised test materials.[33]

In addition, two coherent Raman scattering (CRS) microscopy techniques (stimulated Raman scattering (SRS) and coherent anti-Stokes Raman scattering (CARS)) were applied which allow for test material-specific identification without

the need for extraneous dyes or fluorophores and provide sub-cellular resolution and three-dimensional sectioning capability for visualising the structural features of the test organisms with which the particles interact.[34–36] To date, the CARS technique has been applied to image the uptake, distribution and bioavailability of different nanomaterials (metal oxides, metals, polymers) in human tissues and ecological model species.[34–39] See section 1 of the ESI† for further details on the CRS techniques.

Materials and methods

Test material selection using spontaneous and coherent Raman scattering microscopy

Spontaneous Raman spectra (data not shown) were acquired for five preliminary test materials, (1) the aqueous dispersion of a styrene ACP (110 nm-ACP); (2) the aqueous dispersions of a further styrene ACP (ACP-2); (3) an anionic acrylic ester copolymer dispersion containing free carboxyl groups (AAECP); (4) the aqueous dispersion of a straight acrylic copolymer (SACP); and (5) the aqueous dispersion of a polyester-polyurethane elastomer (PPE) (ESI,† Table SI-1). The aqueous polymer dispersions were synthesised by polymerizing different monomers using emulsion polymerization techniques in water. The spontaneous Raman spectra were used to determine the organic test material with the most suitable spectral characteristics for investigation with CRS. They were acquired using a Renishaw RM1000 Raman microscope (RENISHAW, Wooton-Under-Edge, UK) equipped with a 1200-line per mm grating providing a spectral resolution of 1 cm^{-1} and a diode laser providing excitation at 785 nm with up to 300 mW power. A 40× microscope objective lens was used to focus light onto the substrate. The system was calibrated using the Raman band of a silicon wafer at 520 cm^{-1}. Spectral data were acquired using the Renishaw v.1.2 WiRE software.

In these pre-tests, 110 nm-ACP was best suited for CRS microscopy in terms of its differentiation from fairy shrimp or zebrafish tissues. The 110 nm-ACP exhibited a strong CH peak at 3055 cm^{-1}, indicative of a benzene ring, which is typically not a pronounced peak in biological samples. By contrast, in a comparative assessment of the spectral profiles of 110 nm-ACP and unexposed fairy shrimp, the majority of the other pronounced peaks were recorded in either spectral profile (Fig. 1A; *cf.* ESI,† Fig. SI-1).

To verify that the spectral profile of 110 nm-ACP exhibited the same peaks in spontaneous Raman scattering and CRS, a hyperspectral SRS profile was acquired of 110 nm-ACP applied to a glass coverslip (*cf.* ESI,† section 2). Using SRS, a strong peak at 3055 cm^{-1} was also obtained. This confirmed both the suitability of 110 nm-ACP as test material and of the CRS microscopy (Fig. 1B). Further, a hyperspectral profile was obtained from an unexposed wild-type zebrafish embryo (Fig. 1C). There was negligible contribution to the CH stretch region at 3060 cm^{-1}. Consequently, the wavenumber of 3055 cm^{-1} was identified and selected as an ideal Raman shift to detect the ACP test materials in biological samples.

Test materials

In addition to the 110 nm-ACP test material, a smaller sized 80 nm-ACP was produced to assess the influence of particle size on toxicity. Both were produced by BASF SE (Ludwigshafen, Germany). The presence of organic volatile

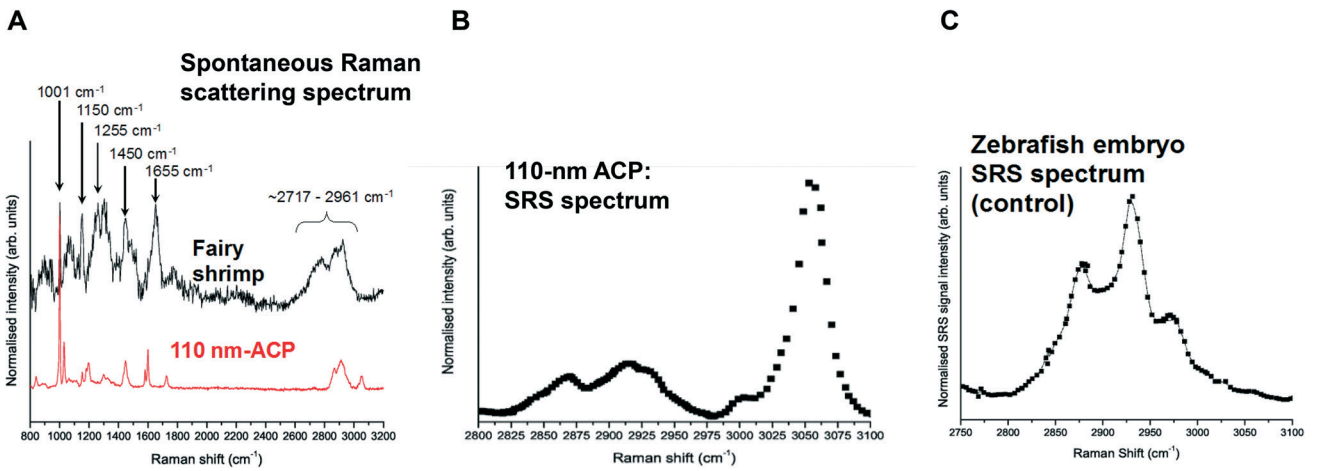

Fig. 1 Spontaneous Raman scattering and stimulated Raman scattering (SRS) profiles of 110-nm ACP, fairy shrimp and zebrafish embryos. A: Spontaneous Raman scattering spectral profiles of a fairy shrimp (black) and 110 nm-ACP. The peaks of the spectral profile of fairy shrimp were tentatively assigned to: 1001 cm^{-1}: phenylalanine; 1150 cm^{-1}: carotenoid (algae); 1255 cm^{-1}: amide III band; 1450 cm^{-1}: CH_2/CH_3; 1655 cm^{-1}: amide I band; 2717–2961 cm^{-1}: CH stretch region. The peaks in the Raman spectrum of Acronal® S790 were tentatively assigned to: 1001 cm^{-1}: aromatic CC band; 1448 cm^{-1}: CH bending for methyl and methylene groups; 1603 cm^{-1}: styrene ring mode; 1731 cm^{-1}: ester carbonyl stretch; 2820–2986 cm^{-1}: CH stretch region; 3055 cm^{-1} aromatic CH stretch. B: SRS hyperspectral profile of 110 nm-ACP applied to a glass coverslip. The hyperspectral profile was generated by successively tuning the pump beam's wavelength thereby yielding a sequence of SRS images which probed the entire CH stretch region of the Raman spectrum. C: SRS hyperspectral profile of an unexposed wild-type zebrafish embryo. The two peaks at approx. 2870 and 2925 cm^{-1} correspond to specific carbon hydrogen bonds.

compounds was assessed by high performance liquid chromatography (HPLC) and gas chromatography (GC). Intrinsic and system-dependent properties of the test materials were assessed using the methods indicated in brackets (as published by Wohlleben and co-workers[40]): primary particle size (transmission electron microscopy (TEM)); particle size distribution (analytical ultracentrifugation (AUC)); volume-specific surface area (VSSA; derived from the AUC-measured particle size distribution); surface chemistry (X-ray photoelectron spectroscopy (XPS)), surface charge (iso-electric potential and zeta potential; zeta sizer), photocatalytic activity (methylene blue method), dispersibility in water (Dulbecco's modified Eagle medium supplemented with 10% foetal calf serum (DMEM/FCS); determined by AUC). Since the test materials were provided as dispersions, specific surface area and dustiness were not determined. The specific styrene ACP has a glass temperature (T_g) of 15.4 °C.

Test organisms and test methods

All animal work and experimental protocols used in this work were approved by the University of Exeter's Animal Welfare and Ethical Review Body, and undertaken under project and personnel licenses granted by the UK Home Office under the United Kingdom Animals (Scientific Procedures) Act and European Law, and in accordance with the University of Exeter's ethical policies.

Overall the experiments were performed in compliance with the relevant national and European Union laws and institutional guidelines, and the responsible institutional committees approved the experiments. Of note, the tests on fairy shrimp are not covered by *Directive 2010/63/EU on the protection of animals used for scientific purposes*.[24] Of the tests using wild-type or zebrafish embryos, only the study parts involving independently feeding forms are covered by this Directive.

Thamnotoxkit F™

Acute toxicity to fairy shrimp (24 h exposure) was determined using the Thamnotoxkit F™ (MicroBioTests Inc., Belgium) according to the manufacturer's instructions.[41] Briefly, the test was performed in 24-well test plates using shrimp larval instars II–III, hatched from dormant eggs, exposed to the test materials and incubated at 26 °C for 24 h in the dark. The number of dead shrimp was recorded, indicated by lack of heart beat, using a stereo dissecting microscope (SMZ-168, Motic®, Germany). At least 90 shrimp were counted for each concentration, *i.e.* 10 shrimp for each of 3 replicates tested in each of 3 independent experiments. Results were expressed as (cumulative) mean mortality ± standard error and LC_{50} values determined. Standardised dilution water served as negative control. Potassium dichromate (Sigma-Aldrich, UK) was used as laboratory positive control.

Fish embryo toxicity (FET) test

A breeding stock of unexposed zebrafish (wild-type WIK strain, originally from the Max Planck Institute, Tubingen, Germany, maintained and bred at the University of Exeter) was used to produce eggs for the FET test that was performed in accordance with OECD TG 236.[20] Briefly, newly fertilised zebrafish eggs were exposed for 96 h, and assessed for viability every 24 h using a stereo dissecting microscope (SMZ-168, Motic®, Germany). The following apical observations were recorded as indicators of toxicity/lethality: (i) coagulation of fertilised eggs; (ii) lack of somite formation; (iii) lack of detachment of the tail-bud from the yolk sac; (iv) lack of heartbeat. Twenty animals were assessed per concentration (3 replicates for each concentration), and LC_{50} values calculated.

Preparation of test materials and range finding tests

Test species were exposed in standardised dilution water prepared according to ISO 7346-3.[42] Stock solutions were prepared by sonicating the test material for 20 seconds, in 2 × 10 second pulses using an ultrasonic probe (6 mm titanium probe, tuned to resonate at 20 kHz ± 50 Hz; Cole-Parmer® 130-Watt Ultrasonic Processors (50/60 Hz, VAC 220), product no. EW-04714-51; Cole-Parmer®, UK) on ice.[43]

The preliminary set of five different polymers (*i.e.* 110 nm-ACP; ACP-2; AAECP; SACP; and PPE) was submitted to range finding studies that were conducted applying the same protocols as the ones described for the main acute aquatic toxicity tests in fairy shrimp and zebrafish. Test material concentrations of 1, 10, 100, 1000 and 10 000 mg L^{-1} (corresponding to 0.0001–1% (v/v)) were assessed in fairy shrimp (24 h exposure; counting 30 animals/concentration) and zebrafish (24, 48, 72 and 96 hpf; 30 animals/concentration). Subsequently, test material concentrations of 1000 and 2500 mg L^{-1} (corresponding to 0.1 and 0.25% (v/v)) were selected for the main tests assessing 80 nm-ACP and 110 nm-ACP. These very high test material concentrations were selected to account for the very low ecotoxicity of the nanoparticle-containing polymer dispersions observed in the range finding studies.

Data evaluation and statistical analysis

The results for the acute aquatic toxicity tests (expressed in mg L^{-1}) were determined based on cumulative counting of two or three independent experiments using Regression Probit analysis with SPSS Statistics for windows version 21.0. Statistical significance was calculated by ANOVA with SPSS Statistics for windows version 21.0 (SPSS Inc., Chicago, USA). Results were considered significant (*) for $p < 0.05$ and highly significant (**) for $p < 0.01$.

The ecotoxicological relevance of the results from the acute toxicity tests with fairy shrimp and wild-type zebrafish embryos was assessed using the LC_{50} value threshold laid down in Regulation (EC) No 1272/2008 on classification, labelling and packaging of substances and mixtures (CLP)[44] and the United Nations Globally Harmonised System of Classification and Labelling of Chemicals (GHS):[45] LC_{50} values exceeding 100 mg L^{-1} recorded after 48 h exposure to crustaceans or after 96 h exposure to fish (or failure to calculate

LC_{50} values at all due to a lack of mortality) do not result in substance classification for acute aquatic toxicity.

Dietary exposure with *Casper* mutant zebrafish

Feeding studies used food containing either polystyrene beads or the test materials (at concentrations of 0.1–100 g 80 nm-ACP or 110 nm-ACP per kg food). Control food was devoid of any test material supplement. Polystyrene bead-supplemented food was used to optimise the imaging method; polystyrene exhibits an intense, characteristic phenyl ring CH stretching peak at approx. 3050 cm^{-1}. Polystyrene beads (100 nm) were purchased from Sigma-Aldrich (Gillingham, UK) as aqueous suspensions containing 1.8×10^{13} beads per mL. ZM-000 food (particle size: approx. <100 μm; composition: 52.0% protein, 12.0% oil, 8.0% ash, 7.0% moisture and 3.0% fibre) was purchased from Zebrafish Management Ltd. (Winchester, UK). Due to its small particle size, ZM-000 food is suitable for the feeding of early developmental stages of zebrafish.

To prepare food containing polystyrene beads, the surfactant present on the polystyrene beads (proportion of the surfactant: 0.1–0.5%; as specified by the supplier Sigma-Aldrich) was first removed by centrifugation (Beckman Avanti J25, Beckman Coulter, UK; 10 min at 17 000 rpm). Next, 4 mL beads were re-suspended in 4 mL standardised dilution water, and added to 4 g ZM-000 food to yield 9×10^{12} particles per gram of food. Food and beads were mixed thoroughly to form a paste, spread on baking sheets and dried for 24 h at 60 °C and ground to a fine powder.

Food containing the ACP test material was prepared by adding equal volumes of the test material preparations in standardised dilution water (0–20%) to equal weights of food to yield final test material concentrations of 0.01, 0.1, 1 and 10% in the food (corresponding to 0.1, 1, 10 and 100 g per kg food). Control food was prepared by using only standardised dilution water.

After mixing, the test material-supplemented food was further processed by oven drying (60 °C; 24 h) or by air drying (~21 °C; 48 h). Oven-dried and air-dried food showed no difference in hyperspectral profile, hence oven drying was used forthwith.

Embryos were collected from a breeding stock of *Casper* zebrafish and individual embryos placed in single wells of a 24-well plate with 2 mL of standardised dilution water, changed every 24 h. For each exposure concentration, 15 embryos were used. The plate was maintained at 26 ± 1 °C, and embryos kept under a constant artificial dark/light cycle of 8/16 h. Ninety-six h post fertilisation (hpf) and 120 hpf, embryos were fed with a fine pipette tip of control food or food containing either the polystyrene beads or the ACP test material (two feedings, each, on either day; for technical reasons, it was not possible to calculate the specific amount fed to the embryos). After each feeding, the water in the wells was changed. At 120 hpf, the feeding studies were terminated immediately after the fry stopped feeding.

Microscopy

Chemically selective imaging by CRS microscopy (implemented as SRS and CARS) was performed as previously established and published.[34–39,46] Section 1 of the ESI† provides further information relevant for the study rationale.

Operational parameters of the combined SRS–CARS microscopy that was applied to produce hyperspectral images and also pre-tests to determine the laser power tolerance of the biological samples are documented in section 2 of the ESI.† Briefly, scan times of approx. 14 and 20 seconds were necessary to obtain a good signal-to-noise ratio in the CARS and SRS images, respectively. At these scan times, locomotion of the live fairy shrimp resulted in blurred images. Therefore, both the fairy shrimp and the zebrafish were fixed in paraformaldehyde (Sigma-Aldrich) prior to CRS microscopic imaging and mounted on their left sides between glass coverslips using low melting point agarose gel (Thermo Fisher Scientific, UK).

Settings that are very specific to the specimen of this study and to the interpretation of microscopy results (*i.e.* the determination of the limit of detection and pre-tests to optimise the SRS and CARS techniques) are presented below.

Semi-quantitative SRS to determine limit of detection

The detected SRS signal is linearly proportional to the concentration of the molecular bonds being probed, and it further varies linearly with both the pump and Stokes laser beam powers. To determine the lowest detectable concentration of the test material with the setup of the present study (applying all parameters as selected for SRS imaging of the aquatic organisms), hyperspectral profiles across the CH stretch region from 2850 cm^{-1} to 3150 cm^{-1} were generated from 110 nm-ACP successively diluted in standardised dilution water. The detected signal was normalised relative to the water background, and the aromatic CH stretch peak height at 3055 cm^{-1} was measured in the CH stretch region (*cf.* ESI,† section 3 for a step-by-step rationale to calculate the number of test material particles in a given unit of the SRS images).

Pre-tests to optimise the SRS and CARS techniques

In pre-tests to optimise the SRS and CARS techniques, SRS and CARS images were acquired from unexposed fairy shrimp (at 20-fold magnification) to determine which anatomical regions of the unexposed animals yielded strong signals in either technique. The pump and Stokes lasers were tuned to excite contrast from the CH stretch at 2856 cm^{-1} that yielded a peak in the spectral profile of this animal (Fig. 1A).

Further, pre-tests were conducted to optimise test material detection during CARS imaging using fairy shrimp exposed to 1000 mg L^{-1} 110 nm-ACP. CARS images were acquired with the pump and Stokes beams tuned to excite contrast from the CH stretch at 2870 cm^{-1} that yielded a peak in the spectral profile of this animal (Fig. 1C). For comparative reasons, a transmitted light image was acquired simultaneously.

Results

Test material characterisation

Table 1 presents the outcome of the physico-chemical characterisation of 80 nm-ACP and 110 nm-ACP (*cf.* ESI,† Table SI-1 for characterisation of ACP-2, AAECP, SACP and PPE). Both test materials appeared as stable, white, milky aqueous dispersions. Using TEM, mean particle sizes of 80 ± 5.8 nm and 112 ± 8.1 nm were measured for 80 nm-ACP and 110 nm-ACP, respectively. The test materials retained complete stability in water, dispersed as individual particles. This results in an average agglomeration number (AAN) equalling 1. For such low AAN, nanomaterial grouping frameworks[5,6] highlight the need to further investigate potential mobility (*i.e.* uptake and bioavailability) – as undertaken in the present study. In the TEM images of dried polymer dispersion, the face-centred cubic (honeycomb) lattice arrangement of polymer particles was observed that is typical for rather monodisperse colloids that are film-forming due to their low T_g (Fig. 2).

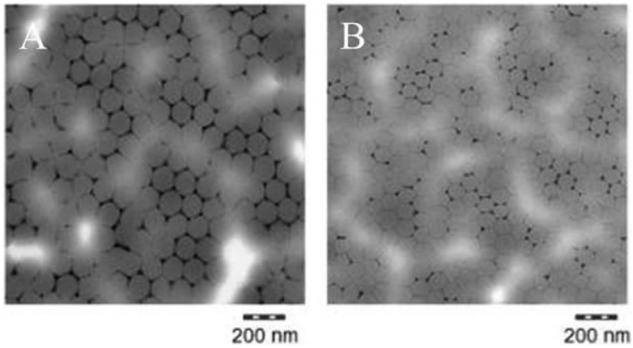

Fig. 2 Transmission electron microscopy (TEM) images of (A) 110 nm-ACP and (B) 80 nm-ACP. Monolayers of particles on TEM grids were prepared by 1 : 100 dilution with deionized water, then dipping the TEM grid into the liquid and drying. Polymers were stained by uranylacetate.

Acute toxicity tests using fairy shrimp and zebrafish embryos

Details on the quality control values of the acute aquatic toxicity tests (*i.e.* dissolved oxygen and pH values of the test material preparations) are provided in section 4 and Table SI-2 of the ESI.†

In the range finding studies with fairy shrimp (ESI,† Fig. SI-2A–SI-2E), none of the initial five test materials showed any toxicity after 24 h exposure at concentrations between 1 and 100 mg L^{-1}, *i.e.* up to the GHS/CLP threshold of 100 mg L^{-1} for acute aquatic toxicity.[44,45] The 110 nm-ACP and AAECP caused no mortality at either 1000 or 10 000 mg L^{-1}. The PPE induced significant mortality at 10 000 mg L^{-1} ($p <$ 0.01) and ACP-2 and SACP at 1000 and 10 000 mg L^{-1} ($p < 0.5$ and < 0.01). In the main experiments, no fairy shrimp (0 of

Table 1 Physico-chemical characterisation of the nanoparticle-containing acrylic copolymer dispersions

Property	Method	Units	80 nm-ACP	110 nm-ACP
Physical appearance			Aqueous dispersion of acrylic copolymer; stable, white, milky; glass temperature: 15.4 °C	
Volatile organic components	HPLC//GC	mg kg^{-1}	Acrylamide: 190; acrylate: 470//*n*-butyl acrylate: 410; styrole: 10; acetone: 110; *n*-butanol: 210; *n*-butyl propionate: 50; *t*-butanol: 180; dibutyl ether: 230; total (GC): 1500	Acrylamide: 8; acrylate: 700//*n*-butyl acrylate: 50; *n*-butanol: 280; *n*-butyl propionate: 20: dibutyl ether: 90; total (GC): 550
Primary particle size (mean)	TEM	D_{50} (nm)	80 ± 5.8	112 ± 8.1
Volume specific surface area	Derived from AUC in H_2O	m^2 cm^{-3a}	49	56
Particle size/dispersibility (H_2O)[b]	AUC	D_{50} (nm)	77.4	107
Particle size/dispersibility (DMEM/FCS)[b]	AUC	D_{50} (nm)	95.4	123
Photocatalytic activity	Methylene blue test	without unit	5.5×10^{-4}	5.0×10^{-4}
Surface chemistry	XPS with carbon line shape analysis	Atom-%	CC, CH: 62.9; CN, C–O: 16.5; COOR: 5.6; O: 14.2; N: 0.3; Si: 0.1; S: 0.1	CC, CH: 62.8; CN, C–O: 16.4; COOR: 5.3; O: 14.6; N: 0.6; Si: 0.1; S: 0.1; Na: 0.1
Iso-electric point	Electrophoretic mobility titration	pH	<3	<3
Zeta-potential at pH 7.4		mV	−60	−56

Abbreviations: AUC: analytical ultracentrifugation; DMEM/FCS: Dulbecco's modified Eagle medium supplemented with 10% fetal calf serum; GC: gas chromatography; HPLC: high performance liquid chromatography; LD: laser diffraction; TEM: transmission electron microscopy; XPS: X-ray photoelectron spectroscopy. Not determined (organic material): crystallite size and crystallite phase; water solubility. Not determined (suspension): surface area by method of Brunauer Emmett and Teller; dustiness (not expected for suspension). [a] As described by Wohlleben and co-workers,[71] the VSSA is an integral property of materials, and it is obtained by dividing the samples' external surface (S) by its solid volume (V) or by multiplying the specific surface area (SSA, surface per mass) by the materials skeletal density (ρ). It is conventionally stated in units of m^2 cm^{-3}. [b] Near perfect stability in serum-containing media; complete stability (dispersed to individual particles) in water.

90 animals) died following exposure to 1000 mg L^{-1} 80 nm-ACP, and 2 of 90 animals died following exposure to 2500 mg L^{-1} 80 nm-ACP. Inter-assay variability is shown in the data (ESI,† Fig. SI-3). Following exposure to 1000 and 2500 mg L^{-1} 110 nm-ACP, a similarly low number of fairy shrimp died (0–7 animals/90 animals at either concentration; ESI,† Fig. SI-4). Thus, for both 80 and 100 nm-ACP, it was not possible to calculate an LC_{50} value (ESI,† Fig. SI-3 and SI-4). Inter-assay variability was higher for the 110 nm-ACP than for the smaller sized 80 nm-ACP.

In range finding studies with zebrafish embryos (ESI,† Fig. SI-5), 110 nm-ACP, AAECP, and PPE showed no effects on survival after 24-, 48-, 72- or 96 h exposure at 1–10 000 mg L^{-1}. ACP-2 and SACP caused significant mortality in zebrafish after 24-, 48-, 72- or 96 h exposure at concentrations of 10 000 mg L^{-1} (100-fold higher than the GHS/CLP threshold of 100 mg L^{-1} for acute aquatic toxicity).[44,45] In the main experiments, neither 1000 nor 2500 mg L^{-1} 80 nm-ACP or 110 nm-ACP caused mortality in zebrafish embryos up to 96 hpf, and it was not possible to calculate an LC_{50} (data not shown). At all test concentrations, flocs of particulate test material were recorded surrounding the chorion, but the embryos developed normally.

Limit of detection for test materials using SRS

Based on the hyperspectral profiles generated from successive dilutions of 110 nm-ACP across the CH stretch region from 2850–3150 cm^{-1}, 0.005 weight% 110 nm-ACP in standardised dilution water was determined as the limit of detection (ESI,† Fig. SI-6). This corresponds to 50 mg L^{-1} 110 nm-ACP. Hence, in the hyperspectral SRS images, each pixel revealing the characteristic 3055 cm^{-1} peak corresponds to a test material concentration of 50 mg L^{-1}.

SRS and CARS spectral profiling of fairy shrimp and zebrafish embryo in acute toxicity tests

In unexposed fairy shrimp, strong signals were detected in the head regions of the animals, and specifically in the eyes and ocelli (simple eyes), both when generating SRS and CARS spectral profiles. These signals are attributed to the pigments present in these organs (Fig. 3). In the preliminary tests conducted on fairy shrimp exposed to 1000 mg L^{-1} 110 nm-ACP, it was not possible to determine precisely which specific region of the fairy shrimp contained the test material (60-fold magnification, Fig. 4 and 5). The strategy adopted for CARS imaging in the main study therefore was to generate several overlapping depth stacks combined with lower magnification images to determine the precise location of the regions of interest within the animals.

SRS hyperspectral images generated from the yolk sac of an unexposed wild-type zebrafish (Fig. 6) and from the yolk sac of a wild-type zebrafish embryo exposed to 1000 mg L^{-1} 80 nm-ACP (Fig. 7), generated at a depth of approx. 3 μm, clearly differ with respect to the spectral features of the 2820–2986 cm^{-1} CH-stretch region. For the zebrafish embryo exposed to 1000 mg L^{-1} 80 nm-ACP, the hyperspectral profile in Fig. 7 exhibits a peak at 3005 cm^{-1} that is attributed to the CH stretch of C=C groups, a marker for the degree of unsaturation of lipids. In the false colour rendering of the hyperspectral data set, this peak appears as discrete droplets with diameters ranging from 2–5 μm which can be interpreted to be lipid droplets that are more unsaturated than the surrounding features. Further, the lipid-rich regions of the yolk sac of the zebrafish embryos that were exposed to 80 nm-ACP (Fig. 7) exhibited a higher degree of unsaturation than the corresponding regions of the yolk sac of the unexposed zebrafish (Fig. 6).

The hyperspectral profile in Fig. 7 also shows a very small, broad peak at 3055 cm^{-1} corresponding to water-rich regions of the sample. Such a peak may be attributable to endogenous amino acids, such as tyrosine or phenylalanine, although these amino acids are more commonly associated with protein-rich regions (such as cell nuclei), and are not commonly seen within lipid droplets. The hyperspectral profile also shows an elevation at 3055 cm^{-1}. Whilst this could be attributed to the benzene CH stretch of 80 nm-ACP, an elevation at 3055 cm^{-1} was also observed in the hyperspectral

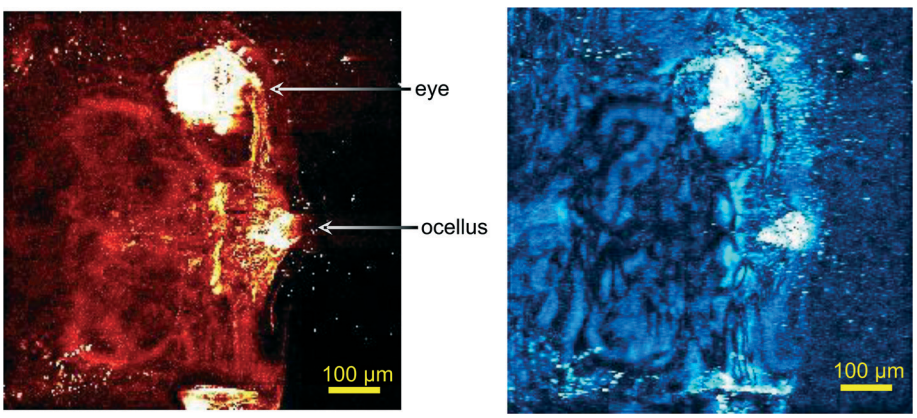

Fig. 3 CARS images (left) and SRS images (right) of the head regions of unexposed fairy shrimp (20-fold magnification). For imaging, the pump and Stokes beams were tuned to excite contrast at 2856 cm^{-1} (CH stretch).

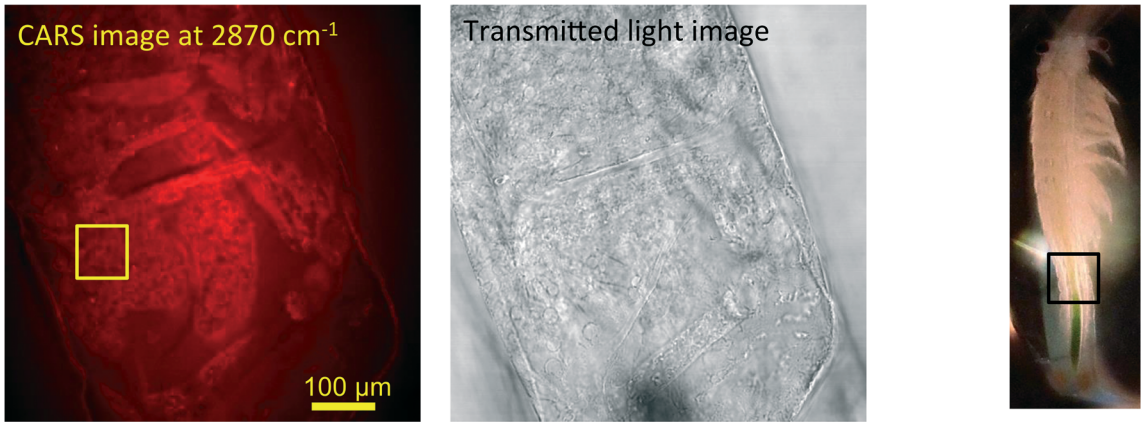

Fig. 4 CARS and transmitted light images of fairy shrimp exposed to 1000 mg L^{-1} 110 nm-ACP. Left image: Epi-detected CARS images were acquired with the pump and Stokes beams tuned to excite contrast from the CH stretch at 2870 cm^{-1}. For Fig. 5, a second set of images was acquired from the region marked with a yellow square to determine whether signals from 110 nm-ACP were detectable at the higher magnification. Middle image: Simultaneously acquired transmitted light image of fairy shrimp exposed to 1000 mg L^{-1} 110 nm-ACP (both: 20-fold magnification). Right image: The region of interest was selected, as indicated by the black box on the fairy shrimp image.

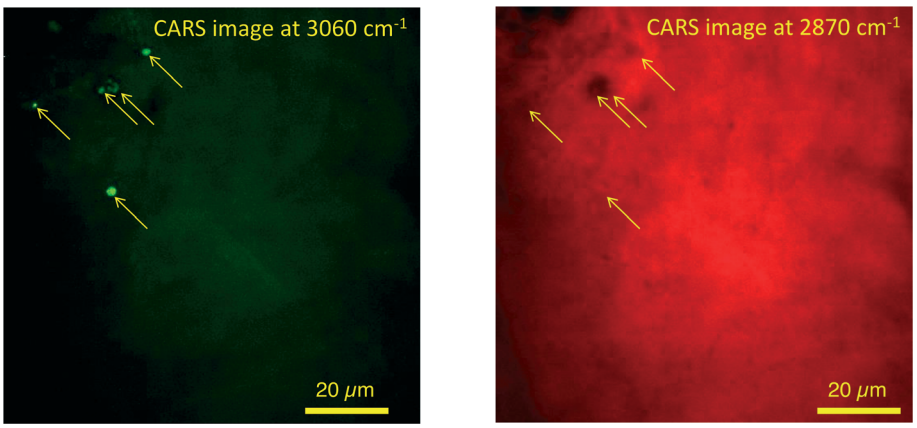

Fig. 5 CARS images of fairy shrimp exposed to 1000 mg L^{-1} 110 nm-ACP (60-fold magnification). These images were obtained from the yellow insert indicated in the left-hand image of Fig. 4. The pump and Stokes beams were tuned to excite contrast from (left image) the aromatic CH stretch at 3060 cm^{-1} and (right image) the CH stretch at 2870 cm^{-1}.

data set of the control animal. The elevation at 3055 cm^{-1} is more pronounced in the hyperspectral profile of the exposed animal, but it is clearly also present in the control animal (Fig. 6). Hence, based upon the 3055 cm^{-1} aromatic CH stretch, we could not say for certain that 80 nm-ACP was taken up into the yolk sac.

SRS spectral profiling and light microscopy analyses of *Casper* mutant zebrafish in dietary exposure studies

SRS spectral profiles confirmed that polystyrene beads could be detected by their characteristic phenyl ring stretch (Fig. 8). Fish food devoid of polystyrene beads did not exhibit a signal from the phenyl ring CH stretch (Fig. 9; left hand image), despite the fact that the food contained a wide range of ingredients, the exact constituents of which are not disclosed by the manufacturers. In the spectral profiles of the polystyrene bead-spiked food, the CH peaks observed between 2820–2986 cm^{-1} were assessed as arising from the food itself (Fig. 9; right hand image), and these peaks were much weaker than the high 3049 cm^{-1} peak elicited by polystyrene beads (Fig. 8). When the polystyrene beads were mixed with food, the phenyl ring CH stretch shifted from 3049 cm^{-1} to a slightly higher peak position (3056 cm^{-1}). This shift may have been caused by a change in the local chemical environment caused when the samples were oven dried. The benzene ring possesses multiple stretching modes between 3040 and 3070 cm^{-1}, and the exact proportion of each of these modes in any one sample depends on the local chemical environment. Hence, the central peak of the phenyl ring CH stretch mode can shift between pure polystyrene beads and polystyrene beads forming part of a mixture. For the test materials, since the ACP dispersions were dried during the processing of the food, film formation of the polymers may have occurred. Therefore, we cannot exclude the possibility that the test materials were no longer present in the form of nanoparticles.

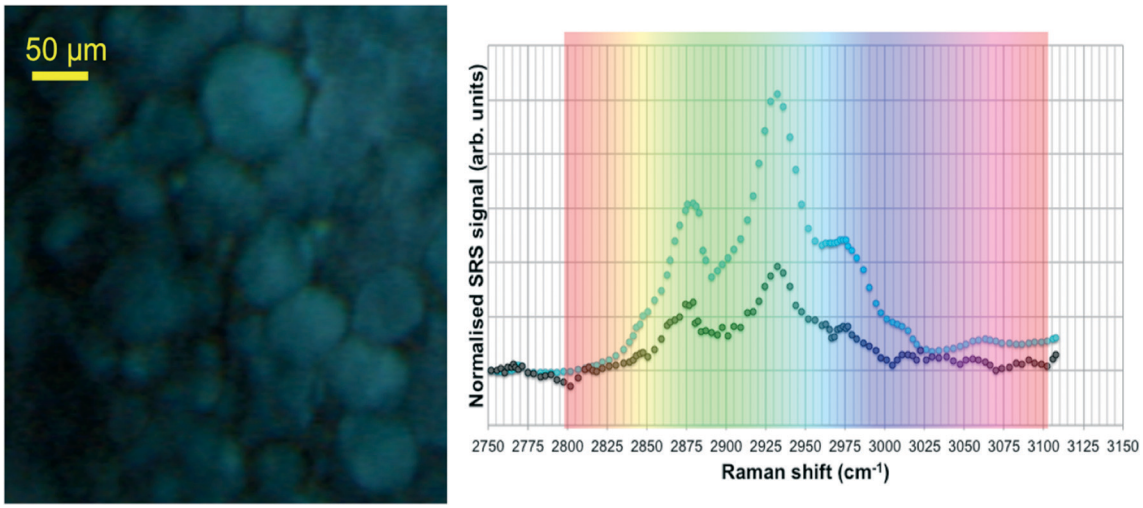

Fig. 6 SRS hyperspectral data acquired from the yolk sac of an unexposed zebrafish embryo, taken from a region approx. 3 μm below the sac's surface. Left: False-colour rendering of the hyperspectral data set (*i.e.* red-green-blue image), where each image was assigned a different colour depending on the corresponding Raman shift. Right: Spectral profiles of two regions of the sample, combined with the 'rainbow' lookup table that was used to generate the false-colour rendering. The black and purple data points correlate with the black and purple regions of the image, respectively.

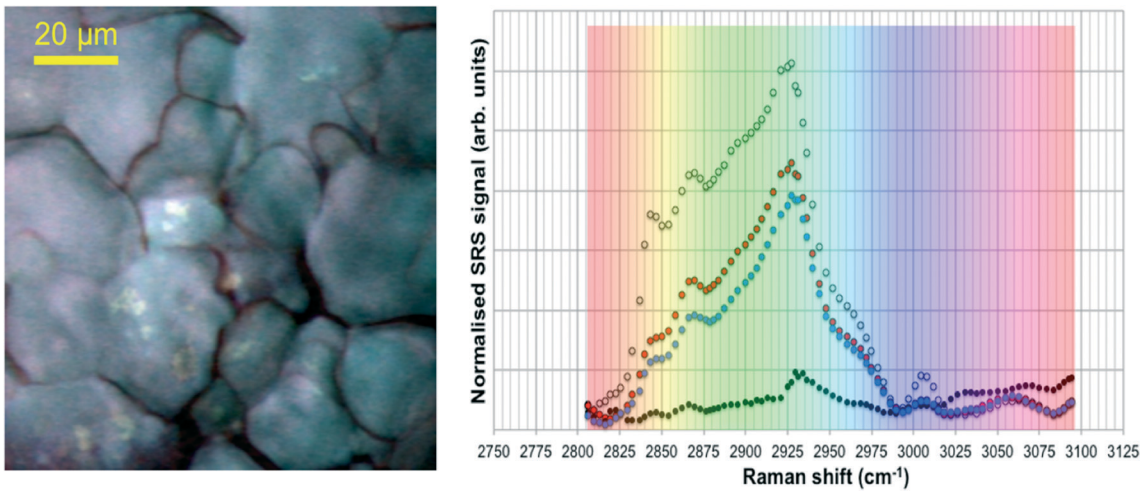

Fig. 7 SRS hyperspectral data acquired from a zebrafish embryo yolk sac exposed to 1000 mg L^{-1} 80 nm-ACP, taken from a region approx. 3 μm below the sac's surface (60-fold magnification). Left: False-colour rendering of the hyperspectral data set (*i.e.* red-green-blue image), where each frame was assigned a different colour depending on the corresponding Raman shift. Right: Spectral profiles of several regions of the sample, combined with the 'rainbow' lookup table that was used to generate the false-colour rendering. The white, red, blue and black data points correlate with the white, red, blue and black regions of the image, respectively.

Hyperspectral SRS data sets acquired from *Casper* zebrafish fed with food spiked with polystyrene beads or control food are provided in Fig. 10. The hyperspectral profile generated from the fish fed with polystyrene bead-containing food exhibits the characteristic CH stretch peak in the yolk region of the fry, indicating the presence of polystyrene beads (Fig. 10A). This peak was not observed in the fish that were fed with the control food (Fig. 10B). The hyperspectral SRS profile of fish food spiked with 0.1 g kg^{-1} 110 nm-ACP or 80 nm-ACP showed a prominent peak located at 3055 cm^{-1}, which correlates well with the CH stretch peak from benzene rings in the spectral profile of the test materials (Fig. 11). This reveals that the test material was present in the fish food. However, it could not be ascertained that it continued to prevail in the form of nanoparticles after the drying procedure. When dried, polymer chains from neighbouring particles, due to their T_g below room temperature, start to interdiffuse, first forming necks between particles and ultimately forming a continuous film.[2]

Light microscopic images of *Casper* zebrafish fed with food containing 0.1–100 g kg^{-1} 80 nm-ACP showed that the fry fed freely on the supplemented food irrespective of the test material concentrations (Fig. 12). Similar results were obtained when the food was supplemented with 110 nm-ACP

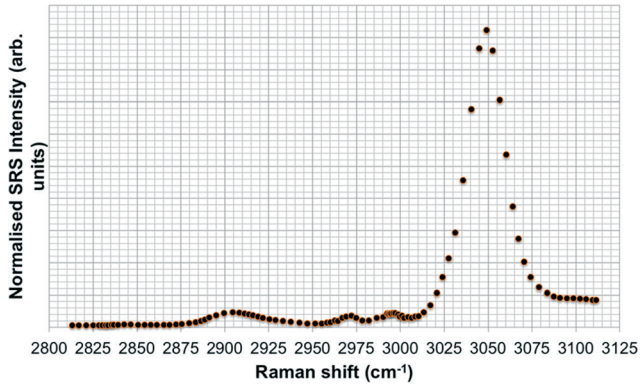

Fig. 8 SRS hyperspectral profile of polystyrene beads taken of the CH stretch region from 2800–3120 cm^{-1}.

(data not shown). Hyperspectral SRS data of *Casper* zebrafish fed with food dosed with an extremely high concentration of 10 g kg^{-1} 80 nm-ACP indicated the characteristic test material peak at around 3055 cm^{-1} in the gut region, albeit only for a total of 5 pixels (Fig. 13; *cf.* Fig. SI-8 and SI-9† for details on the identification of regions of the *Casper* zebrafish that contain the test material signal).

Hyperspectral data sets were acquired from the liver, muscle tissue, intestines, and the surrounding agarose gel of *Casper* zebrafish fed with food spiked with 1 g kg^{-1} 80 nm-ACP or 110 nm-ACP. Signals relating to 80 nm-ACP (*i.e.* the characteristic benzene stretch at 3055 cm^{-1}) were recorded in the liver and intestines, but not in the muscle tissue (Fig. 14). Similarly, 110 nm-ACP (*i.e.* the characteristic benzene stretch at 3055 cm^{-1}) was presumably recorded within the liver (quantity unknown), but not in the muscle tissue or agarose gel surrounding the sample (Fig. 15).

Discussion

In the present study, nanoparticle-containing ACP dispersions were tested for the first time in two aquatic model species, fairy shrimp and zebrafish embryos. Acute toxicity upon aquatic and dietary exposure was assessed. Neither 80 nm-ACP nor 110 nm-ACP elicited acute aquatic toxicity in either

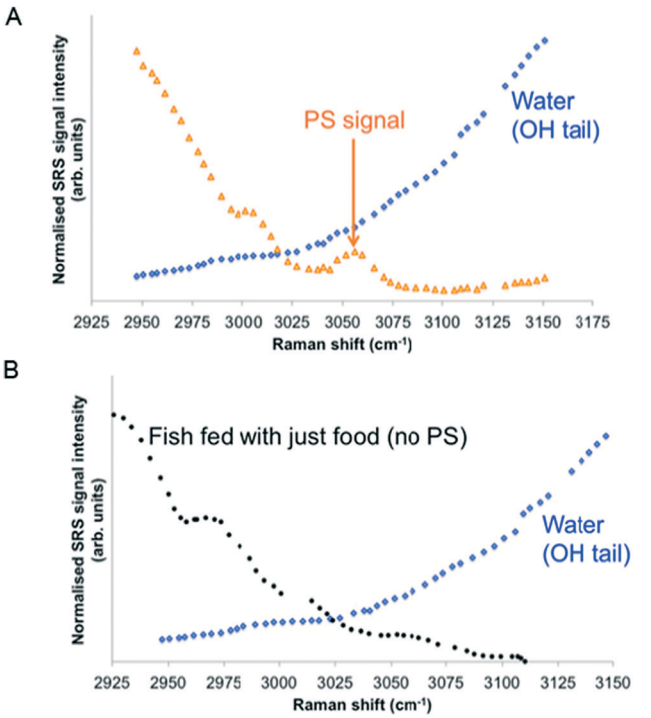

Fig. 10 SRS hyperspectral data sets from *Casper* zebrafish fed with (A) food spiked with polystyrene (PS) beads and (B) control food. The blue data points correspond to spectral points associated with the water-rich agarose gel mounting medium. The black data points (bottom) correspond to yolk from the control fish and do not exhibit any contribution from a phenyl ring CH stretch. The orange data points (top) were generated from the yolk region and exhibit the characteristic phenyl ring CH stretch peak, indicating the presence of PS beads in this region of the fish.

fairy shrimp or zebrafish embryos at exposures bearing any environmental relevance. Mortality was only recorded at very high concentrations (1000 and 2500 mg L^{-1}) that exceed the GHS/CLP threshold of 100 mg L^{-1} to distinguish acute aquatic toxicity from non-classification by 10- and 25-fold.[44,45] These very high test material concentrations were selected for the main experiments after range findings studies confirmed that the test materials have negligible acute aquatic toxicity in fairy shrimp and zebrafish embryos.

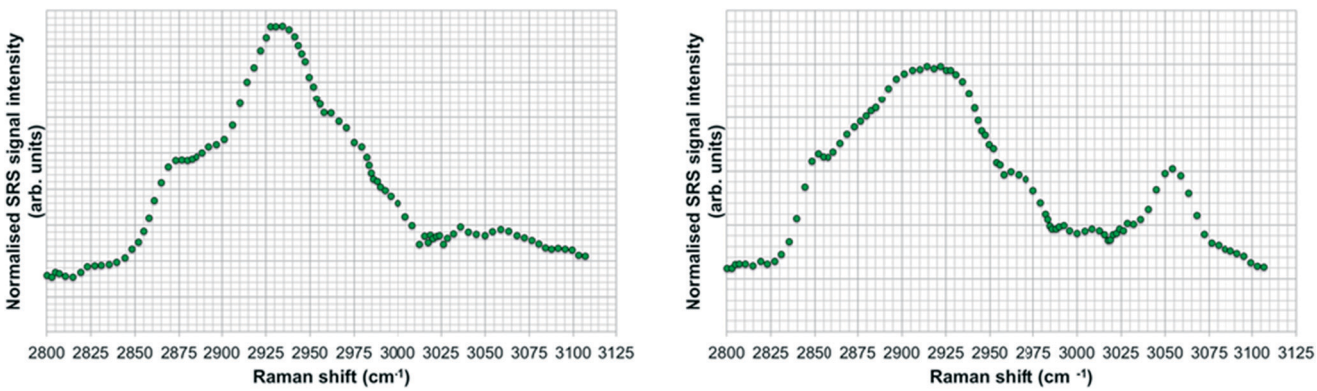

Fig. 9 SRS hyperspectral profiles of fish food without polystyrene beads (left); and of fish food spiked with polystyrene beads (right).

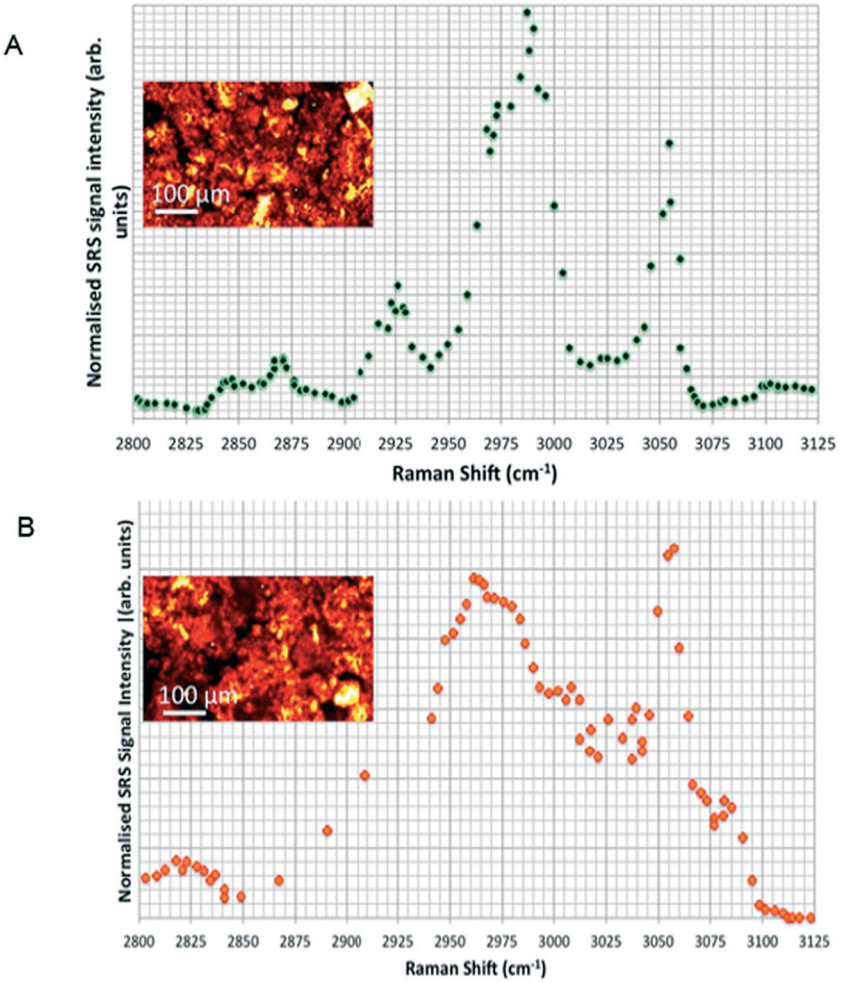

Fig. 11 Hyperspectral SRS profiles of fish food spiked with (A) 0.1 g kg^{-1} 110 nm-ACP or (B) 0.1 g kg^{-1} 80 nm-ACP. The inset images are CARS data sets acquired by tuning the pump and Stokes wavelengths to probe the CH_2 Raman resonance at 2845 cm^{-1} (20-fold magnification).

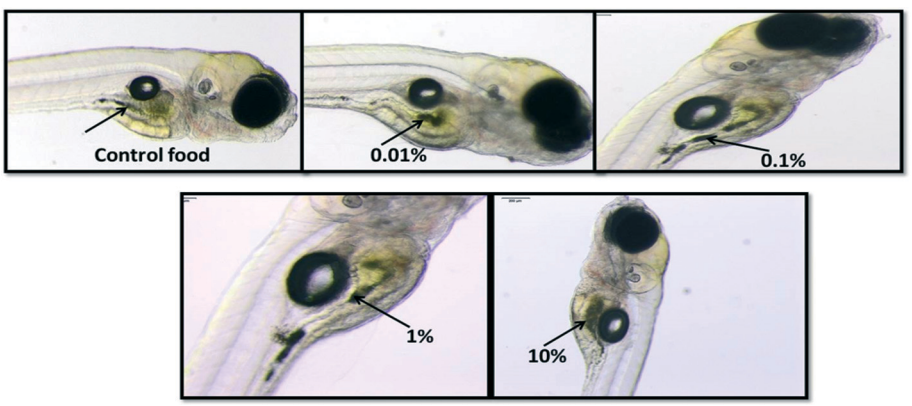

Fig. 12 Light microscopy images of *Casper* zebrafish fry fed with control food or food dosed with 0.1–100 g kg^{-1} food 80 nm-ACP. The arrows point to dark areas reflecting the control food or food dosed with the respective concentrations of 80 nm-ACP.

Neither 80 nm-ACP, nor 110 nm-ACP showed any appreciable toxicity in fairy shrimp or zebrafish, and it was not possible to calculate a LC_{50} value. This confirms that the ACP dispersions show no acute aquatic toxicity under the standardised experimental conditions adopted. It is possible that at higher exposure concentrations, the test materials might cause toxic effects by physically adhering to the chorion,[47–50] but such physical effects are most probably not relevant for environmental exposures.

A rapidly increasing number of studies have investigated the potential human health effects of engineered nanomaterials. There have been far fewer studies of their potential

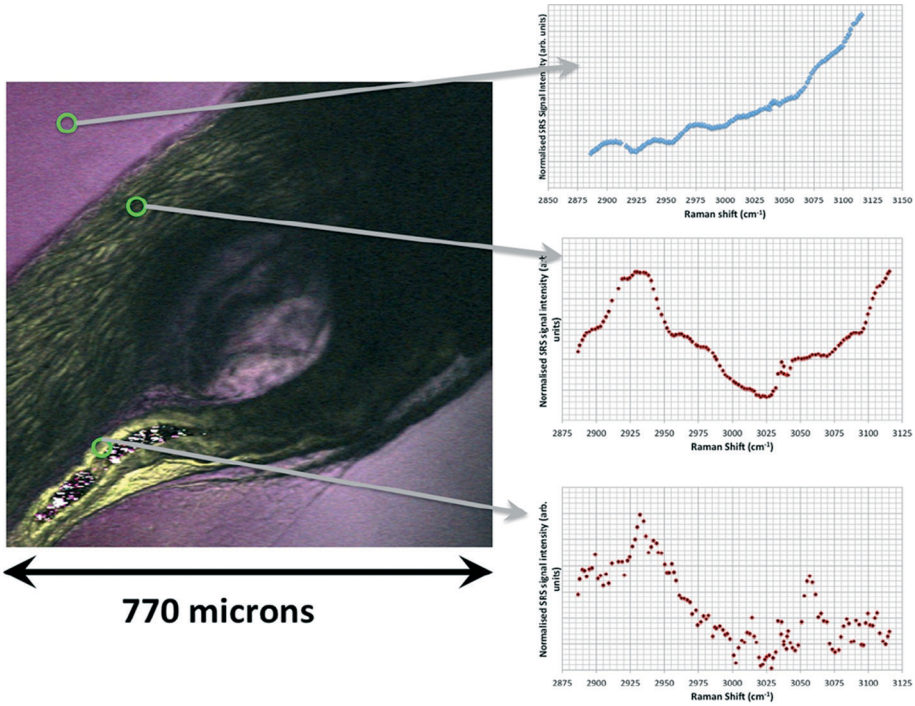

Fig. 13 Hyperspectral data set acquired from a *Casper* zebrafish fed with food spiked with 10 g kg^{-1} 80 nm-ACP at 96 h and 120 h. Left: The SRS composite image is a z-projection of the entire hyperspectral data set, where each frame of the spectrum corresponds to a different colour. One side of the image corresponds to 770 μm. Right: The three spectral profiles were obtained from the respective regions indicated with arrows. • Top: Water-rich Raman spectrum from the agarose gel surrounding the fish. The dominant spectral feature is the high wavenumber OH bond tail. • Middle: Protein-rich spectral profile of muscle tissue, exhibiting a CH_3 peak at 2930 cm^{-1} and a contribution from the OH tail stretch at higher wavenumbers. • Bottom: Characteristic 80 nm-ACP peak at around 3055 cm^{-1} discovered in the gut region, total pixel count: 5.

ecotoxicological effects and these have generally focused on inorganic nanomaterials, *e.g.* metals and metal oxides[51,52] or metalloid oxides, such as amorphous silica nanomaterials.[53,54] Only a few publications consider the ecotoxicology of organic (polymer) nanomaterials, *e.g.* the studies from Naha and co-workers[11] and Besseling and co-workers.[55]

Generally, different nanomaterials induce effects on cells, tissues or organisms through different modes-of-action. For instance, the toxicity of metal and metal oxide nanomaterials is mainly attributable to the effects of the solubilised ions, and effects caused by high-aspect ratio carbon nanotubes follow a fibre toxicity paradigm.[5,6] Evidence is currently lacking for 'nanospecific' effects, which can be attributed to the smallness of the particles alone.[56,57]

This study illustrates that the 24 h acute lethal toxicity test using the Thamnotoxkit F™ (ISO 14380:2011)[19] and the zebrafish FET test (OECD TG 236)[20] are suitable to assess the potential acute aquatic toxicity of organic nanomaterials and nanoparticle-containing polymer dispersions. During regulatory environmental hazard assessment addressing the aquatic compartment, *e.g.* in accordance with the REACH Regulation,[21] this information is relevant together with information on degradation (*e.g.* sediment simulation testing) and fate and behaviour in the environment. Further, information on potential ecotoxicological effects has to be available before test substance uptake and biodistribution can be assessed, because such testing has to be performed at non-toxic concentrations. Nanoparticle agglomeration or dispersibility may alter the effective concentration of nanomaterials within the test systems or target organs in toxicity tests.[58,59] Hence, specific dispersion protocols should be used during nanomaterial preparation to reduce agglomeration. Different methods used to prepare dispersions of the same nanomaterial may account for variations in the outcomes of (eco) toxicity studies.[43]

In the few studies published investigating the effects of inorganic or organic nanomaterials on fairy shrimp, they have proven to be sensitive indicators of ecotoxicity. In a comparative assessment of different metal oxide nanomaterials (primary particle sizes (PPS): 50–70 nm ZnO; 30 nm CuO; 25–70 nm TiO_2), fairy shrimp (*T. platyurus*) were more sensitive than water fleas (*Daphnia magna*).[60] TiO_2 nanomaterials did not show any toxicity up to an extremely high concentration of 20 g L^{-1}, and although toxicity occurred at higher exposure concentrations for zinc oxide and copper oxide nanoparticles this appeared mainly to be driven by the effects of the solubilised metal ions.[60] Exposure (1 h) of *T. platyurus* to aqueous suspensions of 3 and 6 mg L^{-1} fullerene C_{60} and C_{70}, resulted in their ingestion leading to fullerene C_{60} and C_{70} burdens of 2.7 ± 0.4 and 6.8 ± 1.5 mg per mg wet weight, respectively, but without any observable signs of toxicity.[61]

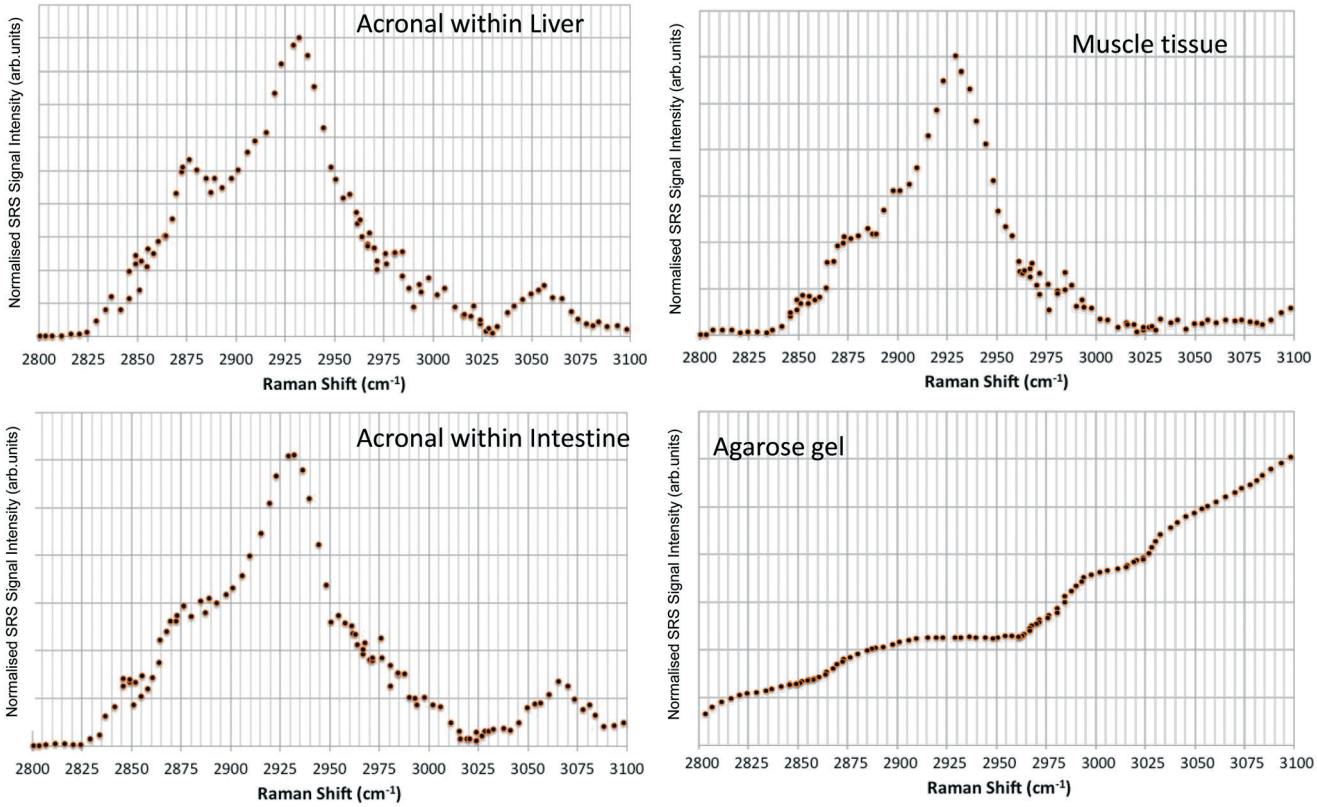

Fig. 14 SRS hyperspectral data sets from a *Casper* zebrafish fed with food spiked with 1 g kg^{-1} 80 nm-ACP. The spectra are acquired from: • Top left: Regions of the liver containing 80 nm-ACP signal; • Top right: muscle tissue; • Bottom left: regions of the intestine containing 80 nm-ACP signal; • Bottom right: the surrounding agarose gel. The characteristic muscle tissue spectral profile presents a strong CH_3 stretch at 2930 cm^{-1} and a contribution to the spectral profile from the OH stretch tail at higher wavenumbers. In order to improve the signal-to-noise ratio for these low-concentration experiments, each frame generated in the hyperspectral stack was the average of 3 successive image acquisitions.

Poly *N*-isopropylacrylamide and *N*-isopropylacrylamide/*N*-*tert*-butylacrylamide copolymer nanoparticles were virtually non-toxic in fairy shrimp, yielding a LC_{50} value of 943 mg L^{-1}.[11] In a test battery of aquatic organisms representing different trophic levels, amorphous silica nanomaterials (PPS: 50 and 100 nm) showed no effects up to 1.0 mg mL^{-1}, whereas polyethyleneimine polystyrene nanomaterials (PPS: 55 and 110 nm) caused acute toxicity at 0.0004–0.42 mg mL^{-1}, with effects generally more pronounced for the 110 nm-, than for the 55 nm test material.[62] In this study, *T. platyurus* was less sensitive than *D. magna*, but more sensitive than *Vibrio fischeri* bacteria.[62]

In brine shrimp (*Artemia franciscana*) larvae, 48 h exposure to 40 nm anionic carboxylated polystyrene nanomaterials or 50 nm cationic amino polystyrene nanomaterials (for both up to 0.1 mg mL^{-1}) did not induce mortality, but larvae exposed to amino polystyrene nanoparticles underwent multiple molting events compared with the control larvae, suggesting a stress response.[63] At 48 h exposure, the test materials were heavily sequestrated in the gut and some material was also adhered to the antennae and appendages, potentially hampering larvae motility.[63]

A broad spectrum of different nanomaterials encompassing metals, metal oxides, metal compounds as well as amorphous silica, calcium and carbon compounds has already been tested in the zebrafish FET test.[52,64] The most pronounced effects have been observed for metal and metal oxide nanomaterials that shed toxic (metal) ions.[52] Generally, the chorion that protects the developing zebrafish embryos is not a barrier for most manufactured non-nanosized or nanosized substances.[65–68] Substances that form complexes or large structures with other similar molecules through chemical interactions, such as ionic bonding (*e.g.* cationic polymers); substances which interact with sulfhydryl groups (*e.g.* heavy metals); or large molecules (*e.g.* polymers) can be blocked by the chorion.[65] By comparison, small 5–46 nm silver (Ag) nanomaterials (at concentrations >0.19 nM) can cross chorion pore channels that have diameters of 0.5–0.7 μm, *via* passive diffusion.[69] Exposure to these small Ag nanomaterials can lead to fin fold abnormalities, tail flexure, cardiac oedema, yolk sac oedema, head oedema, and eye abnormalities.[69] By comparison, studies on fluorescent core–shell silica nanoparticles (PPS: 60 nm and 200 nm) exposed at concentrations between 0.0025 and 200 mg L^{-1} were found to adsorb onto the chorion of zebrafish embryos (at 96 hpf), but were not taken up by the embryos.[53] These materials did not cause mortality or deformities[53] (of note, 200 nm particles are not covered by the definition of

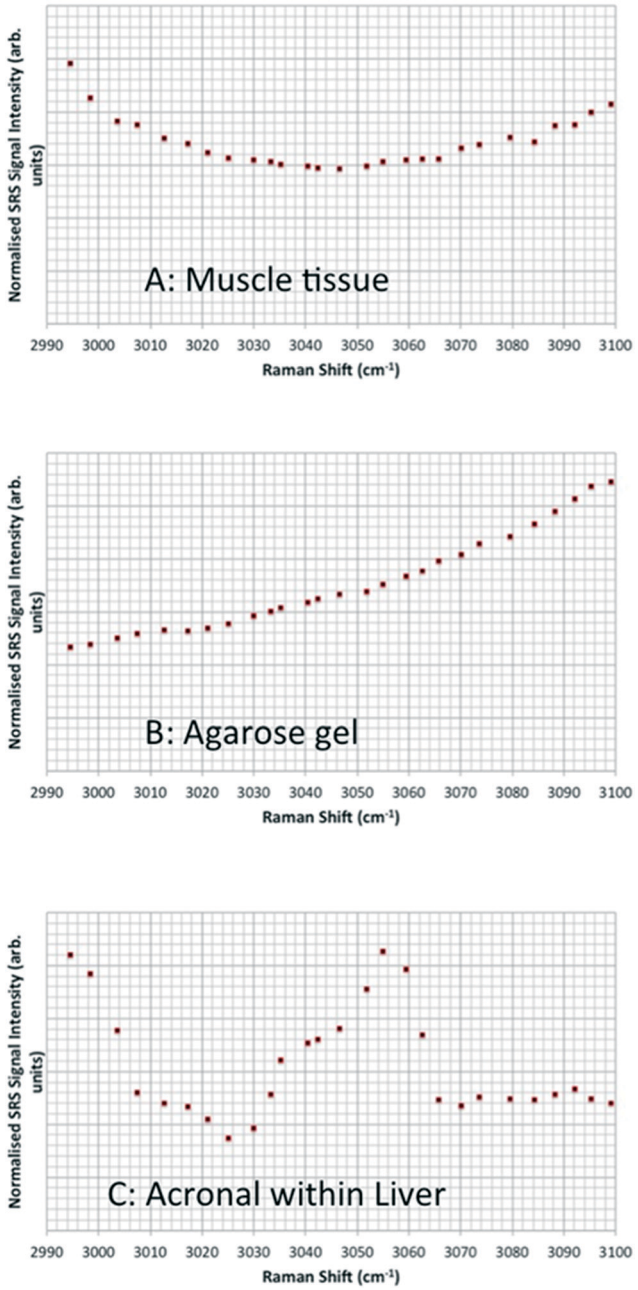

Fig. 15 Hyperspectral data sets from *Casper* zebrafish fed with food spiked with 110 nm-ACP. The profiles exhibit: • (A and B) the "tail" of the OH water stretch at higher wavenumbers; • (A and C) the "tail" of the CH_3 stretch at 2930 cm^{-1}; • (C) the characteristic ACP peak around 3055 cm^{-1}. The hyperspectral stacks for these data were curtailed such that they only encompass the ACP peak region from 2990–3100 cm^{-1} (rather than the entire CH stretch). In order to improve the signal-to-noise ratio for these low-concentration experiments, each frame generated in the hyperspectral stack was the average of 3 successive image acquisitions.

'nanomaterial' as laid down in an EU Commission recommendation[70]).

In another study, exposure to 25–200 μg ml^{-1} amorphous silica nanomaterials (62 nm; without core shell) resulted in a dose-dependent decrease in the hatching rate of zebrafish embryos, and increase in mortality and embryonic malformations, including pericardial oedema, yolk sac oedema, and head malformation.[54] Duan and co-workers[54] did not report if or how the applied amorphous silica interacted with the chorion. Thus, while further investigations are necessary to corroborate our findings, the nanoparticle-containing ACP dispersions we tested do not appear to show any toxic effects of significance in either fairy shrimp or zebrafish embryos. Further, uptake of the test materials into the liver of the *Casper* zebrafish could not be identified with certainty. If such biodistribution is confirmed during future research work, specific investigations of the hepatic metabolism of the test materials would be merited. The major metabolic pathway for the monomers after oral uptake is ester hydrolysis to the alcohol and acrylic acid finally resulting in CO_2. The monomers are eliminated quickly.

This study presents the first example to our knowledge of the application of CRS microscopy to explore the potential ecotoxicology of nanoparticle-containing ACP dispersions and to infer on the uptake and biodistribution of these test materials. Therefore, our study included pre-tests to determine the limit of detection of the test materials using CRS (50 mg L^{-1} 110 nm-ACP), and to optimise the imaging procedure (*i.e.* fixation of the animals in paraformaldehyde; 14–20 seconds scan times; generation of overlapping depth stacks combined with lower magnification images to localise regions of interest within the animals). An advantage of CRS microscopy is that it does not require extensive preparation of the biological samples that may affect the nanomaterials, as is the case for, *e.g.*, TEM or scanning electron microscopy.[36,46] The applicability of CRS microscopy for investigating organic nanomaterials (or larger sized organic materials) is however restricted to organic materials whose spectral profile is clearly distinguishable from the spectral profile of the biological structures under investigation. In the present study, only 1 of 5 originally selected organic polymers had such a distinct spectral peak, *i.e.* the 3055 cm^{-1} aromatic CH stretch.

The CRS images yielded preliminary information on the uptake and biodistribution of nanoparticle-containing ACP dispersions. The hyperspectral profiles of control wild-type zebrafish embryos and embryos exposed to 1000 mg L^{-1} 80 nm-ACP both showed peaks at 3055 cm^{-1}, although the peak was weaker in the control animal. This suggests that endogenous features, such as the amino acids tyrosine and phenylalanine were also contributing to this peak. We could not determine with certainty that 80 nm-ACP penetrated into the yolk sac of zebrafish embryos, and we could not quantify the tissue burden in the test animals. There were nonetheless clear differences between control and test samples within the 2820–2986 cm^{-1} CH stretch region. There are numerous CH stretch peaks that contribute to this profile, overlapping with each other to generate these complex spectral features. It would be interesting to obtain additional spectra to deconvolute these peaks from the measured spectra (*e.g.* by curve fitting) to determine more clearly which components of

the CH stretch region change after exposure to 80 nm-ACP. Such investigations could also investigate how this test material could be affecting lipid composition within the embryo's yolk sac, as is indicated here. This could plausibly be due to physical adherence of the test material to the chorion when applied at high concentrations that may affect (for example) oxygen exchange.

The results from the feeding studies using *Casper* mutant zebrafish provide preliminary results on the uptake, bioavailability and organ distribution of ACP dispersions when spiked in fish food. We show that the ACP dispersions were taken up by the *Casper* zebrafish, with strong indications for their presence in the intestines, as we would expect for dietary expose to any material, and also with preliminary evidence for a presence in the liver. The latter would indicate uptake across the gut and into the circulation, a topic worthy of further investigation. Since ACP are known to fuse when dried, future research should also explore how the intrinsic material properties of the ACP dispersions are affected by different processing techniques, *e.g.* oven heating *versus* air drying.

Conclusions

In conclusion, we show that the nanoparticle-containing ACP dispersions we tested do not possess acute aquatic toxicity in either fairy shrimp or wild-type zebrafish. Notwithstanding, these data do not allow deriving conclusions on potential long-term effects. In the acute aquatic toxicity tests, CRS imaging indicated alterations to lipid composition in the yolk sacs of zebrafish exposed to the test materials, but neither material presence in this tissue nor the possible effect mechanism were established. In feeding studies using *Casper* zebrafish, the test materials were taken up into the gut and possibly liver. It is possible that the nanoparticles were transformed during food preparation so that the animals were exposed to a composite of food and adhering and/or fused ACP nanoparticles. CRS microscopy proved to be a promising method for investigations into the ecotoxicology of organic nanomaterials whose chemical composition is similar to that of the biological samples. The application of these techniques warrants further investigation.

Author contributions

TSG, CRT, YD, NG, DR, and designed carried out, and evaluated the aquatic exposure and dietary studies. NG and JM carried out and evaluated the microscopic studies. WW designed, carried out and evaluated the physico-chemical characterisation of the test materials. TSG, UGS, NG, and YD wrote the manuscript. KW, EL, WW, GS, and RL advised the design of the study and the interpretation of the results. GS supervised the production and characterisation of the test materials. TSG, CRT, KW, and EL supervised the preparation of the manuscript. All authors read and approved the final manuscript.

Conflicts of interest

EL, RL, GS, WW and KW are employees of BASF SE, a company that produces and markets nanomaterials. TSG, YD, NG, DR, CRT, JM received partial funding from BASF SE to design and conduct the study. UGS was hired by BASF SE to assist in the preparation of the manuscript. All authors alone are responsible for the writing and the contents of this article.

Acknowledgements

The study was financed by BASF SE, Ludwigshafen, Germany, and the University of Exeter, Exeter, UK. TG and CRT were additionally supported from NERC grant NE/N006178.

References

1 L. Ma-Hock, R. Landsiedel, K. Wiench, D. Geiger, V. Strauss, S. Gröters, B. van Ravenzwaay, M. Gerst, W. Wohlleben and G. Scherer, *Int. J. Toxicol.*, 2012, **31**, 46–57.
2 EPDLA, European Polymer Dispersion and Latex Association position paper on polymer dispersions and nanotechnology, 14 June 2012, available from: http://www.cefic.org/About-us/How-Are-We-Organised/Cefic-Headquarter/The-Industry-Sectors/Fine-Speciality-and-Consumer-Chemicals/European-Polymer-Dispersion-and-Latex-Association-EPDLA-/.
3 W. J. Stark, P. R. Stoessel, W. Wohlleben and A. Hafner, *Chem. Soc. Rev.*, 2015, **44**, 5793–5805.
4 J. H. Arts, M. Hadi, A. M. Keene, R. Kreiling, D. Lyon, M. Maier, K. Michel, T. Petry, U. G. Sauer, D. Warheit, K. Wiench and R. Landsiedel, *Regul. Toxicol. Pharmacol.*, 2014, **70**, 492–506.
5 J. H. Arts, M. Hadi, M. A. Irfan, A. M. Keene, R. Kreiling, D. Lyon, M. Maier, K. Michel, T. Petry, U. G. Sauer, D. Warheit, K. Wiench, W. Wohlleben and R. Landsiedel, *Regul. Toxicol. Pharmacol.*, 2015, **71**(Suppl 2), S1–S27.
6 J. H. Arts, M. A. Irfan, A. M. Keene, R. Kreiling, D. Lyon, M. Maier, K. Michel, N. Neubauer, T. Petry, U. G. Sauer, D. Warheit, K. Wiench, W. Wohlleben and R. Landsiedel, *Regul. Toxicol. Pharmacol.*, 2016, **76**, 234–261.
7 R. S. Kookana, A. B. Boxall, P. T. Reeves, R. Ashauer, S. Beulke, Q. Chaudhry, G. Cornelis, T. F. Fernandes, J. Gan, M. Kah, I. Lynch, J. Ranville, C. Sinclair, D. Spurgeon, K. Tiede and P. J. Van den Brink, *J. Agric. Food Chem.*, 2014, **62**, 4227–4240.
8 N. C. Mueller and B. Nowack, *Environ. Sci. Technol.*, 2008, **42**, 4447–4453.
9 J. R. Lead and K. J. Wilkinson, *Environ. Chem.*, 2006, **3**, 159–171.
10 S. J. Klaine, P. J. J. Alvarez, G. E. Batley, T. F. Fernandes, R. D. Handy, D. Y. Lyon, S. Mahendra, M. J. McLaughlin and J. R. Lead, *Environ. Toxicol. Chem.*, 2008, **27**, 1825–1851.
11 P. C. Naha, A. Casey, T. Tenuta, I. Lynch, K. A. Dawson, H. J. Byrne and M. Davoren, *Aquat. Toxicol.*, 2009, **92**, 146–154.
12 A. Saber, N. Jacobsen, A. Mortensen, J. Szarek, P. Jackson, A. Madsen, K. Jensen, I. Koponen, G. Brunborg, K. Gutzkow, U. Vogel and H. Wallin, *Part. Fibre Toxicol.*, 2012, **9**, 4.

13 J. P. Kaiser, M. Roesslein, L. Diener and P. Wick, *PLoS One*, 2013, **8**, e83215.
14 S. Rana and P. T. Kalaichelvan, *ISRN Toxicol.*, 2013, **2013**, 574648.
15 J. Liu, J. Katahara, G. Li, S. Coe-Sullivan and R. H. Hurt, *Environ. Sci. Technol.*, 2012, **46**, 3220–3227.
16 T. V. Duncan, *ACS Appl. Mater. Interfaces*, 2014, **7**, 20–39.
17 S. Froggett, S. Clancy, D. Boverhof and R. Canady, *Part. Fibre Toxicol.*, 2014, **11**, 17.
18 W. Wohlleben, S. Brill, M. W. Meier, M. Mertler, G. Cox, S. Hirth, B. von Vacano, V. Strauss, S. Treumann, K. Wiench, L. Ma-Hock and R. Landsiedel, *Small*, 2011, **7**, 2384–2395.
19 International Organization for Standardization ISO 14380:2011, Water quality determination of the acute toxicity to Thamnocephalus platyurus (Crustacea; Anostraca), 2011, available at: http://www.iso.org.
20 Organisation for Economic Co-operation and Development Guidelines for the Testing of Chemicals No 236, Fish embryo acute toxicity (FET) test, OECD, Paris, France, adopted 26 July 2013.
21 Regulation (EC) No 1907/2006 of the European Parliament and of the Council of 18 December 2006 concerning the Registration, Evaluation, Authorisation and Restriction of Chemicals (REACH), establishing a European Chemicals Agency, amending Directive 1999/45/EC and repealing Council Regulation (EEC) No 793/93 and Commission Regulation (EC) No 1488/94 as well as Council Directive 76/769/EEC and Commission Directives 91/155/EEC, 93/67/EEC, 93/105/EC and 2000/21/EC. OJ L, 396, 1, 30 December 2006.
22 Organisation for Economic Co-operation and Development Guidelines for the Testing of Chemicals No 203, Fish, acute toxicity test, OECD, Paris, France, adopted 17 July 1992.
23 W. M. S. Russell and R. L. Burch, The principles of humane experimental technique. London, UK. Methuen, 1959. Reprinted by UFAW, 1992: 8 Hamilton Close, South Mimms, Potters Bar, Herts EN6 3QD England, p. 238.
24 Directive 2010/63/EU of the European Parliament and of the Council of 22 September 2010 on the protection of animals used for scientific purposes, OJ L, 276, 33, 20 October 2010.
25 M. Halder, A. Kienzler, M. Whelan and A. Worth, EURL ECVAM Strategy to replace, reduce and refine the use of fish in aquatic toxicity and bioaccumulation testing. JRC Science and Policy Report, JRC93222, EUR 26973 EN, 2014.
26 C. B. Kimmel, W. W. Ballard, S. R. Kimmel, B. Ullmann and T. F. Schilling, *Dev. Dyn.*, 1995, **203**, 253–310.
27 G. N. Wheeler and A. W. Brändli, *Dev. Dyn.*, 2009, **238**, 1287–1308.
28 J. Xu, B. P. Srinivas, S. Y. Tay, A. Mak, X. Yu, S. G. P. Lee, H. Yang, K. R. Govindarajan, B. Leong, G. Bourque, S. Mathavan and S. Roy, *Genetics*, 2006, **174**, 735–752.
29 S. Scholz, S. Fischer, U. Gündel, E. Küster, T. Luckenbach and D. Voelker, *Environ. Sci. Pollut. Res.*, 2008, **15**, 394–404.
30 S. Scholz, N. Klüver and R. Kühne, Analysis of the relevance and adequateness of using Fish Embryo Acute Toxicity (FET) Test Guidance (OECD 236) to fulfil the information requirements and addressing concerns under REACH. Report ECHA-UFZ contract ECHA/2014/341, 2016, available at: https://echa.europa.eu/documents/10162/13639/fet_report_en.pdf (accessed February 2017).
31 C. H. Eriksen and R. J. Brown, *Crustaceana*, 1980, **39**, 11–21.
32 C. H. Eriksen and B. Belk, *Fairy shrimps of California's puddles, pools, and playas*, Mad River Press, Eureka CA, USA, 1999.
33 L. I. Zon and R. T. Peterson, *Nat. Rev. Drug Discovery*, 2005, **4**, 35–44.
34 J. Moger, B. D. Johnston and C. R. Tyler, *Opt. Express*, 2008, **16**, 3408–3419.
35 T. Galloway, C. Lewis, I. Dolciotti, B. D. Johnston, J. Moger and F. Regoli, *Environ. Pollut.*, 2010, **158**, 1748–1755.
36 H. J. Butler, L. Ashton, B. Bird, G. Cinque, K. Curtis, J. Dorney, K. Esmonde-White, N. J. Fullwood, B. Gardner, P. L. Martin-Hirsch, M. J. Walsh, M. R. McAinsh, N. Stone and F. L. Martin, *Nat. Protoc.*, 2016, **11**, 664–687.
37 T. M. Scown, R. M. Goodhead, B. D. Johnston, J. Moger, M. Baalousha, J. R. Lead, R. van Aerle, T. Iguchi and C. R. Tyler, *Environ. Chem.*, 2010, **7**, 36–49.
38 N. Garrett, M. Whiteman and J. Moger, *Opt. Express*, 2011, **19**, 17563–17574.
39 A. Lalatsa, N. L. Garrett, T. Ferrarelli, J. Moger, A. G. Schätzlein and I. F. Uchegbu, *Mol. Pharmaceutics*, 2012, **9**, 1764–1774.
40 W. Wohlleben, L. Ma-Hock, V. Boyko, G. Cox, H. Egenolf, H. Freiberger, B. Hinrichsen, S. Hirth and R. Landsiedel, *J. Ceram. Sci. Technol.*, 2013, **4**, 93–104.
41 Thamnotoxkit F™, Crustacean toxicity screening test for freshwater, Standard Operational Procedure, Creasel, Deinze, Belgium, 1995, p. 23.
42 International Organization for Standardization ISO 7346–3, Water quality - Determination of the acute lethal toxicity of substances to a freshwater fish [Brachydanio rerio Hamilton-Buchanan (Teleostei, Cyprinidae)], Flow-through method, 1996, available at: http://www.iso.org.
43 N. B. Hartmann, K. A. Jensen, A. Baun, K. Rasmussen, H. Rauscher, R. Tantra, D. Cupi, D. Gilliland, F. Pianella and J. M. R. Sintes, *J. Toxicol. Environ. Health, Part B*, 2015, **18**, 299–326.
44 Regulation (EC) No 1272/2008 of the European Parliament and of the Council of 16 December 2008 on classification, labelling and packaging of substances and mixtures, amending and repealing Directives 67/548/EEC and 1999/45/EC, and amending Regulation (EC) No 1907/2006, OJ L, 353, 1–1355, 31 December 2008.
45 United Nations Globally Harmonized System of Classification and Labelling of Chemicals (GHS), 6th revised edition, United Nations, New York, USA, and Geneva, CH, ST/SG/AC.10/30/Rev.6, 2015.
46 R. M. Goodhead, J. Moger, T. S. Galloway and C. R. Tyler, *NANO*, 2015, **9**, 928–939.
47 J. P. Grierson and A. C. Neville, *Tissue Cell*, 1981, **13**, 819–830.
48 R. D. Podolsky, *J. Exp. Biol.*, 2002, **205**, 1657–1668.
49 S. F. Perry, M. Ekker, A. P. Farrell and C. J. Brauner, *Fish physiology: Zebrafish*, Academic Press, San Diego CA, USA, 2010, ISBN: 9780123749833.

50 R. Strecker, T. B. Seiler, H. Hollert and T. Braunbeck, *Comp. Biochem. Physiol., Part C: Toxicol. Pharmacol.*, 2011, **153**, 318–327.
51 K. Wiench, W. Wohlleben, V. Hisgen, K. Radke, E. Salinas, S. Zok and R. Landsiedel, *Chemosphere*, 2009, **76**, 1356–1365.
52 J. A. Kovriznych, R. Sotnikova, D. Zeljenkova, E. Rollerova, E. Szabova and S. Wimmerova, *Interdiscip. Toxicol.*, 2013, **6**, 67–73.
53 K. Fent, C. J. Weisbrod, A. Wirth-Heller and U. Pieles, *Aquat. Toxicol.*, 2010, **100**, 218–228.
54 J. Duan, Y. Yu, H. Shi, L. Tian, C. Guo, P. Huang, X. Zhou, S. Peg and Z. Sun, *PLoS One*, 2013, **8**, e74606.
55 E. Besseling, B. Wang, M. Lürling and A. A. Koelmans, *Environ. Sci. Technol.*, 2014, **48**, 12336–12343, DOI: 10.1021/es503001d; erratum in: Environ Sci Technol, 2 Dec 2014, 48, 14065.
56 K. Donaldson and C. A. Poland, *Curr. Opin. Biotechnol.*, 2013, **24**, 724–734.
57 R. Landsiedel, U. G. Sauer, L. Ma-Hock, J. Schnekenburger and M. Wiemann, *Nanomedicine*, 2014, **9**, 2557–2585.
58 G. DeLoid, J. M. Cohen, T. Darrah, G. Pyrgiotakis, W. Wohlleben and P. Demokritou, *ACS Nano*, 2014, **5**, 3514.
59 J. M. Cohen, G. M. DeLoid and P. Demokritou, *Nanomedicine*, 2015, **10**, 3015–3032.
60 M. Heinlaan, A. Ivask, I. Blinova, H.-C. Dubourguier and A. Kahru, *Chemosphere*, 2008, **71**, 1308–1316.
61 M. Patra, X. Ma, C. Isaacson, D. Bouchard, H. Poynton, J. M. Lazorchak and K. R. Rogers, *Environ. Toxicol. Chem.*, 2010, **30**, 828–835.
62 M. P. Casado, A. Macken and H. J. Byrne, *Environ. Int.*, 2013, **51**, 97–105.
63 E. Bergami, E. Bocci, M. L. Vannuccini, M. Monopoli, A. Salvati, K. A. Dawson and I. Corsi, *Ecotoxicol. Environ. Saf.*, 2016, **123**, 18–25.
64 O. J. Osborne, B. D. Johnston, J. Moger, M. Balousha, J. R. Lead, T. Kudoh and C. R. Tyler, *NANO*, 2013, **7**, 1315–1324.
65 K. Henn, Limits of the fish embryo toxicity test with *Danio rerio* as an alternative to the acute fish toxicity test, *PhD Thesis*, Combined Faculties for the Natural Sciences and for Mathematics of the Ruperto-Carola University of Heidelberg, Germany, 2011, p. 103.
66 L. Yang, N. Y. Ho, R. Alshut, J. Legradi, C. Weiss, M. Reischl, R. Mikut, U. Liebel, F. Müller and U. Strähle, *Reprod. Toxicol.*, 2009, **28**, 245–253.
67 S. Basu and C. Sachidanandan, *Chem. Rev.*, 2013, **113**, 7952–7980.
68 T. Braunbeck, B. Kais, E. Lammer, J. Otte, K. Schneider, D. Stengel and R. Strecker, *Environ. Sci. Pollut. Res.*, 2015, **22**, 16247–16261.
69 K. J. Lee, P. D. Nallathamby, L. M. Browning, C. J. Osgood and X.-H. Xu, *ACS Nano*, 2007, **1**, 133–143.
70 Commission recommendation on the definition of nanomaterial. OJ L, 275, 38, 18 October 2011.
71 W. Wohlleben, J. Mielke, A. Bianchin, A. Ghanem, H. Freiberger, H. Rauscher, M. Gemeinert and V. D. Hodoroaba, *J. Nanopart. Res.*, 2017, **19**, 61.